

Contribution from the Department of Chemistry, University of Florence, Florence, Italy, Departement de Recherche Fondamentale, Centre d'Etudes Nucleaires, Grenoble, France, and Institut d'Electronique Fondamentale, Orsay, France

Magnetic Phase Transition and Low-Temperature EPR Spectra of a One-Dimensional Ferrimagnet Formed by Manganese(II) and a Nitronyl Nitroxide

Andrea Caneschi,^{1a} Dante Gatteschi,^{*1a} Jean Pierre Renard,^{1b} Paul Rey,^{*1c} and Roberta Sessoli^{1a}

Received July 29, 1988

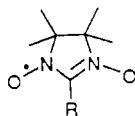
The magnetic properties of single crystals of the chain compound formed by manganese(II) hexafluoroacetylacetonate and the nitronyl nitroxide radical NIT-*i*-Pr (NIT-*i*-Pr = 2-isopropyl-4,4,5,5-tetramethyl-4,5-dihydro-1*H*-imidazolyl-1-oxyl 3-oxide), Mn(hfac)₂NIT-*i*-Pr, have been investigated at low temperature to characterize the magnetic phase transition. Measurements at low magnetic field (0-1 Oe) reveal that the system undergoes a transition to a 3-D ferromagnetic ordered state at 7.6 K. The observed magnetic anisotropy is of the *XY* type in agreement with a calculation of the dipolar energies. The dipolar interaction seems to be the origin of the phase transition as confirmed also by the value of the critical exponent $\gamma = 1.13$. The single-crystal EPR spectra recorded in the range of temperature 4.2-300 K show the effect of short-range order with the resonance field depending on the crystal orientation. The *g* shifts are related to the magnetic susceptibility extending to the case of ferrimagnetic chains the model previously suggested by Nagata and Tazuke for one-dimensional ferro- and antiferromagnets. Mn(hfac)₂NIT-*i*-Pr is found to behave as the typical one-dimensional ferrimagnet.

Introduction

Magnetic phase transitions in molecular materials are currently being actively investigated,²⁻¹⁵ both from a fundamental point of view, with the aim to individuate novel magnetic behaviors, different from those of the traditional magnets based on metal or ionic lattices, and also with the perspective to eventually synthesize new magnetic materials that can be used in the so-called molecular electronics.

The main results obtained so far are ferromagnetic phase transitions observed in lattices formed by one-dimensional ferromagnets and ferrimagnets, which occur at temperatures below 20 K. Claims of high-temperature phases have not yet been adequately substantiated, and their actual existence is dubious.

We are trying to synthesize new magnetic materials using as building blocks metal ion complexes such as hexafluoroacetylacetonates, M(hfac)₂, and pentafluorobenzoates, M(pfbz)₂, and stable organic radicals such as the nitronyl nitroxides, NITR, whose general formula is¹⁶



- (1) (a) University of Florence. (b) Institut d'Electronique Fondamentale. (c) Centre d'Etudes Nucleaires.
- (2) Miller, J. S.; Epstein, A. J.; Reiff, W. M. *Acc. Chem. Res.* **1988**, *21*, 114.
- (3) Mataga, N. *Theor. Chim. Acta* **1968**, *10*, 372.
- (4) Ovchinnikov, A. A. *Theor. Chim. Acta* **1978**, *47*, 297.
- (5) Sugawara, T.; Bandow, S.; Kimura, K.; Iwamura, H.; Itoh, K. *J. Am. Chem. Soc.* **1986**, *108*, 368.
- (6) Izuoka, A.; Murata, S.; Sugawara, J.; Iwamura, H. *J. Am. Chem. Soc.* **1985**, *107*, 1786.
- (7) Torrance, J. B.; Oostra, S.; Nazzari, A. *Synth. Met.* **1987**, 709.
- (8) Pei, Y.; Verdager, M.; Kahn, O. *J. Am. Chem. Soc.* **1986**, *108*, 7428.
- (9) Pei, Y.; Verdager, M.; Kahn, O.; Sletten, J.; Renard, J. P. *Inorg. Chem.* **1987**, *26*, 138.
- (10) Le Page, J. J.; Breslow, R. *J. Am. Chem. Soc.* **1987**, *109*, 6412.
- (11) Korshak, Yu.; Medvedeva, T. V.; Ovchinnikov, A. A.; Spektor, V. N. *Nature (London)* **1987**, *326*, 370.
- (12) Miller, J. S.; Epstein, A. J. *J. Am. Chem. Soc.* **1987**, *109*, 3850.
- (13) Caneschi, A.; Gatteschi, D.; Renard, J. P.; Rey, P.; Sessoli, R. *J. Am. Chem. Soc.* **1989**, *111*, 785.
- (14) Coronado, E.; Drillon, M.; Fuertes, A.; Beltran, D.; Mosset, A.; Galy, J. *J. Am. Chem. Soc.* **1986**, *108*, 900.
- (15) Kahn, O.; Pei, Y.; Verdager, M.; Renard, J. P.; Sletten, J. *J. Am. Chem. Soc.* **1988**, *110*, 782.
- (16) Caneschi, A.; Gatteschi, D.; Laugier, J.; Rey, P.; Sessoli, R.; Zanchini, C. In *Organic and Inorganic Low Dimensional Crystalline Materials*; Delhaes, P., Drillon, M., Eds.; NATO ASI Series; Plenum: New York, 1987; p 381.

These radicals have one unpaired electron, which is delocalized on the two equivalent N-O groups.

With these we obtained both ferromagnetic and ferrimagnetic chains^{17,18} and other low-dimensional systems that undergo magnetic phase transitions at 20-25 K.¹³

In particular manganese(II) hexafluoroacetylacetonate, Mn(hfac)₂, forms one-dimensional materials in which a NITR (R = methyl, ethyl, propyl, and phenyl) radical bridges two different manganese ions and each metal ion is bound to two different radicals (see Figure 1). The high-temperature magnetic behavior, which has been already discussed,¹⁸ is typical of one-dimensional ferrimagnets, as shown by the magnetic susceptibility and the EPR spectra. The manganese ions, $S = 5/2$, and the radicals, $S = 1/2$, were found to be antiferromagnetically coupled with *J* in the range 210-330 cm⁻¹, depending on the radical. Throughout the paper we use the spin Hamiltonian in the form $H = \sum_{i < j} J_{ij} \hat{S}_i \cdot \hat{S}_j$. The high values of χT at low temperature and the log χ vs log *T* plots induced us to suspect that a magnetic phase transition occurs at temperatures close to 5-10 K. Since the understanding of the factors determining the occurrence of three-dimensional order is of paramount importance in the design of new bulk ferro- or ferrimagnets, we have performed experiments in low external magnetic fields on Mn(hfac)₂NIT-*i*-Pr with the purpose of characterizing the magnetic phase transition and we wish to report them here, together with low-temperature EPR spectra that show apparent short-range order effects, providing first-hand information on the preferred spin arrangement.

Experimental Section

The synthesis of the adduct formed by Mn(hfac)₂ and radical NIT-*i*-Pr (NIT-*i*-Pr = 2-isopropyl-4,4,5,5-tetramethyl-4,5-dihydro-1*H*-imidazolyl-1-oxyl 3-oxide), Mn(hfac)₂NIT-*i*-Pr, and the structure determination have already been reported.¹⁸ The compound crystallizes in the monoclinic system, space group *P*2₁/*c*. The crystals used in EPR and magnetic measurements were oriented by using an Enraf-Nonius CAD4 four-circle diffractometer and were found to have largely developed (100) and $(\bar{1}00)$ faces.

Variable-temperature single-crystal EPR spectra in the range 4.2-300 K were recorded with a Bruker ER200 spectrometer operating at X-band frequency and equipped with an Oxford Instruments ESR9 continuous-flow cryostat.

The magnetic moment of single crystals glued on monocrystalline platelets of silicon was measured by using a low-field SQUID magnetometer¹⁹ in the temperature range 4.2-11 K with different experimental procedures. In field-cooled (FC) magnetization, the sample is cooled below its critical temperature, *T*_c, in the field applied above *T*_c. In

- (17) Caneschi, A.; Gatteschi, D.; Laugier, J.; Rey, P. *J. Am. Chem. Soc.* **1987**, *109*, 2191.
- (18) Caneschi, A.; Gatteschi, D.; Rey, P.; Sessoli, R. *Inorg. Chem.* **1988**, *27*, 1756.
- (19) Beauvillain, P.; Chappert, C.; Renard, J. P. *J. Phys. E* **1985**, *18*, 839.

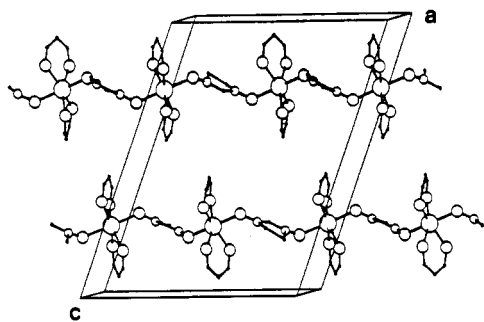


Figure 1. Schematic view of the content of the unit cell of $\text{Mn}(\text{hfac})_2\text{NIT-}i\text{-Pr}$. The cell dimensions are $a = 20.135 \text{ \AA}$, $b = 9.430 \text{ \AA}$, $c = 15.475 \text{ \AA}$, and $\beta = 110.74^\circ$.

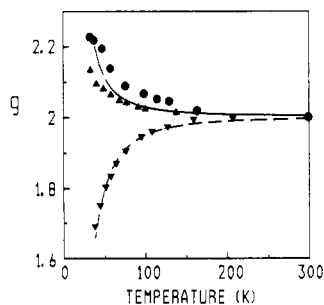


Figure 2. Experimental g values observed at three different crystal settings: (\blacktriangle) parallel to a^* ; (\bullet) parallel to b ; (\blacktriangledown) parallel to c . The lines correspond to g_{\parallel} (---) and g_{\perp} (—) calculated as described in the text by using the parameters $J = 313 \text{ cm}^{-1}$ and $D = 0.06 \text{ K}$.

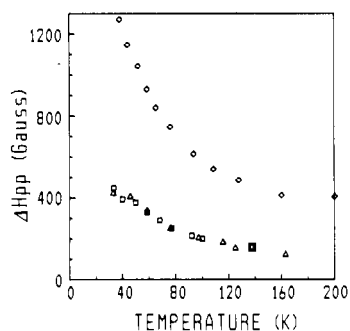


Figure 3. Temperature dependence of EPR line width along the a^* (\square), b (\blacktriangle), and c (\diamond) axes.

zero-field-cooled (ZFC) magnetization, the sample is cooled in zero field (less than 1 mOe in our apparatus), the field is applied at a temperature $T \ll T_c$, and the measurements are performed at increasing temperatures. In remnant magnetization, the sample is cooled in the applied field below T_c , the field is then suppressed, and the magnetization is measured at increasing temperatures.

Hysteresis loops were recorded by a conventional fluxmetric method at $T = 4.2$ and 1.2 K .

Results

Single-crystal EPR spectra of $\text{Mn}(\text{hfac})_2\text{NIT-}i\text{-Pr}$ were recorded with the static magnetic field parallel to the a^* , b , and c crystal axes of the monoclinic cell, which within error coincide with the principal axes. The resonance fields were found to be temperature dependent as shown in Figure 2. In particular when the static magnetic field is parallel to c , the resonance shifts to high field, while it goes downfield in the ab plane. The maximum downfield shift is observed parallel to b . The sum of the g shifts is close to zero. Below 20 K the line width grows so large that its precise measurement is difficult, and closer to the transition temperature effects due to three-dimensional critical fluctuation are visible. The temperature dependence of the line width parallel to the a^* , b , and c axes is shown in Figure 3. The line widths are found to increase on decreasing temperature, but the effect is much more marked parallel to c (the chain direction) compared to the other two directions. As a consequence the angular de-

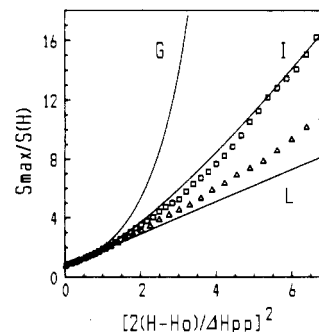


Figure 4. Analysis of the line shape along the c axis at room temperature (\square) and at 125 K (Δ). The lines correspond to Gaussian (G) and Lorentzian (L) line shapes. $S(H) = (Y(H)/(H - H_0))^{1/2}$, where Y is the amplitude of the derivative of the absorption.

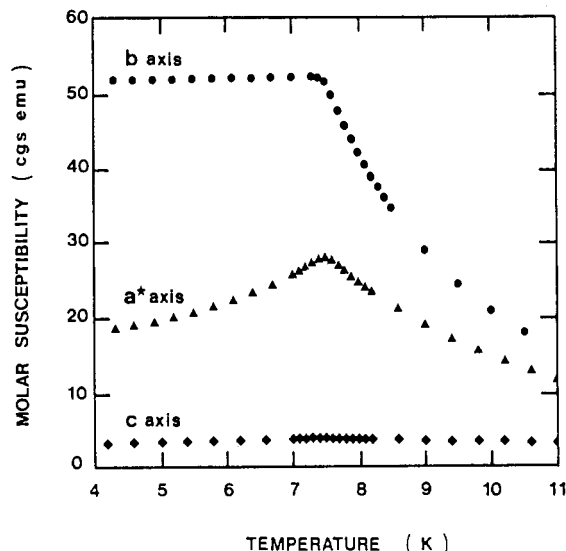


Figure 5. Magnetic susceptibility per mole of oriented crystals measured in an external field of 0.5 Oe .

pendence of the line width at low temperature is different from that observed at room temperature, moving from a $(3 \cos^2 \theta - 1)^{4/3}$ to a $(1 + \cos^2 \theta)$ dependence, where θ is the angle of the external magnetic field with the chain direction.

Also the line shape is temperature dependent as shown in Figure 4. Along the chain direction the line is diffusive at room temperature;²⁰ i.e., it corresponds to the Fourier transform of $\exp(-t^{3/2})$, while on cooling it goes closer to the Lorentzian limit.

The single-crystal magnetic susceptibility was measured in fields of 0.5 Oe along the a^* , b , and c axes in the range $4.2\text{--}11 \text{ K}$. Since the crystals were not large enough to allow measurements on one individual, nine isooriented crystals were used. The crystals have the shape of platelets elongated along the c direction, and the maximum misalignment can be roughly estimated to be on the order of 5° . The results are shown in Figure 5. A magnetic phase transition occurs at $T \approx 7.6 \text{ K}$, with the easy axis parallel to b , a^* being the intermediate axis. The temperature independence of the susceptibility along the easy axis below the transition temperature is due to demagnetization effects and is typical of a ferromagnet. The demagnetizing factor can be evaluated as 7.94 from the present data and is substantially in accord with the shape of the sample even if accurate calculations cannot be performed.

The anisotropy fields can be estimated by extrapolating to 0 K the observed susceptibilities along the intermediate and hard axes, respectively, and correcting for the demagnetization effects. The calculated values are $H_{\text{anis}}(a^*) = 1200 \text{ G}$ and $H_{\text{anis}}(c) = 7500 \text{ G}$. No irreversibility effects are observed above 4.5 K , since in

(20) Richards, P. M. In *Local Properties at Phase Transition*; Editrice Compositori: Bologna, Italy, 1975.

this range the FC and ZFC curves are practically superimposable.

In order to determine accurately the transition temperature T_c , and the critical behavior, more accurate measurements were performed along the easy axis with points collected every 0.01 K in the range 7.5–8.1 K. The susceptibility, corrected for the demagnetizing field, follows the critical law

$$\chi = \Gamma(T - T_c)^\gamma$$

The γ parameter was obtained through linear regression applied to the equation

$$\log \chi_{\text{cor}} = -\gamma \log t + C$$

where $t = (T - T_c)/T_c$ and χ_{cor} is the value of the susceptibility corrected for the demagnetizing effect. The best-fit values are $T_c = 7.61$ K and $\gamma = 1.13$, with the agreement factor $r = 0.99992$.

Saturation measurements were performed on polycrystalline samples in external fields up to 500 Oe. The largest observed value of the magnetization, 13 260 emu mol⁻¹ G, corresponds to a complete saturation of crystallites with the easy axis parallel to the field and a partial saturation of those with the intermediate and hard axes, in agreement with the nature of the sample and the calculated anisotropy fields. The complete saturation expected for the $S = 2$ spin of a manganese–radical pair antiferromagnetically coupled is 22 330 emu mol⁻¹ G.

A hysteresis loop measured at 1.2 K showed only a very small residual magnetization, on the order of 1% of that measured in the highest field, which decays with time.

Discussion

The observed transition to three-dimensional order has a ferromagnetic nature. The anisotropy is essentially of the XY type, with the easy plane orthogonal to the chain direction, as concurrently indicated by the magnetic anisotropy and the EPR data. Actually the XY plane is slightly anisotropic and the preferred spin orientation is parallel to b , which corresponds to the shortest interchain contacts, 943 pm. Beyond two chains related by translations parallel to b , each chain has two pairs of nearest neighbors at 1022 and 1038 pm (the distance corresponds to the shortest contacts between manganese ions). There is no obvious exchange pathway between the chains, because the manganese ions are shielded by the hfac molecules and the shortest contact between oxygen atoms of nitroxides belonging to different chains is 787 pm. Therefore, it seems probable that any interchain coupling constant J' is indeed very small compared to the intrachain coupling constant J , which has been evaluated by using a classic–quantum spin model to be 329.8 cm⁻¹.^{18,21} This is confirmed also by the high-temperature EPR spectra, which are very close to the ideal one-dimensional behavior.

The observed magnetic anisotropy is most probably dipolar in nature since the exchange interaction is expected to be isotropic in a system containing manganese(II), an S ion, and an organic radical. The calculation of the dipolar interaction in systems like these is by no means trivial, because the unpaired electron on the radicals is not localized on any particular atom but, rather, is spread out on all the molecule. Further, when we consider the nearest-neighbor interaction between manganese and the radical within the chain, we recognize that the distance between the spins (the Mn–O distance is 220 pm) is not large compared to their spatial distribution, so that the point dipolar approximation breaks down. However, MO calculations on model metal–nitroxide species,²² which take into account the wave functions of the interacting spins, have shown that the energy of the dipolar interaction can be reasonably estimated with a point dipolar approach that puts one spin on the manganese and the other roughly halfway between the nitrogen and oxygen atom of the nitroxide, even for Mn–O distances as short as 220 pm. For a nitronyl nitroxide such as the one in the present compound, approximate calculations of the dipolar interaction can be performed by splitting the radical spin on the two N–O groups and setting half an electron on each

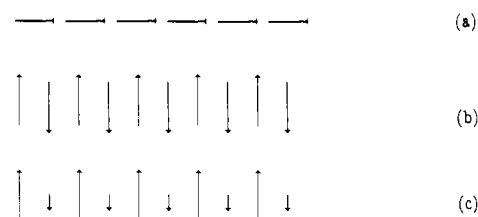


Figure 6. Preferred spin orientations in an ideal one-dimensional ferromagnet (a), antiferromagnet (b), and ferrimagnet (c).

of the two positions halfway between the nitrogen and oxygen atoms. We calculated the interaction of the magnetic moments placed on the manganese ion and on the radical with the other moments enclosed in a shell of given radius for three different spin arrangements. The calculations were repeated iteratively for different values of the radius in steps of 100 pm up to 800 pm, when the calculated value did not vary significantly from that of the previous shell. The total number of included spins is 4622. The manganese spins are parallel to each other and antiparallel to those of the radicals; the direction of alignment of the spins has been considered as coincident with the a^* , b , and c axes, respectively, in the three cases. We found that the most stable configuration is that in which the spins are oriented in the plane perpendicular to the chain direction, in agreement with the experimental data. The calculated energies per mole are $E_{D\parallel} = +0.26$ K and $E_{D\perp} = -0.13$ K, where the symbols indicate the direction of the spin alignment referred to the chain direction. These values are largely determined by the intrachain interaction as shown by calculations that neglected the interchain contribution.

The critical temperature is expected to be related to the dipolar energy and to the intrachain exchange coupling.²³ For Heisenberg chains it was found that $T_c = K(|E_{D\parallel}|/J)^{1/2}$, where K is a constant close to 1 and J is the intrachain coupling constant.²⁴ In the present case we calculate $T_c = 7.9$ K, in good agreement with the experimental value. Therefore, the preferred spin orientation and the lack of any reasonable exchange pathway between the chains suggest that the origin of the ferromagnetic transition is essentially the dipolar interaction, in agreement with the critical exponent calculated from the experimental data. In fact, the observed value $\gamma = 1.13$ indicates a behavior that is closer to the uniaxial dipolar ferromagnet ($\gamma \cong 1$) than to the Heisenberg 3-D ferromagnet ($\gamma = 1.38$).²³ The relatively high transition temperature is determined by the strong intrachain coupling constant, which keeps the spins largely oriented at relatively high temperatures, as shown by the correlation length, which at 20 K is on the order of 30 manganese–radical units.

The shifts of the resonance fields observed in the EPR spectra at low temperature are due to short-range correlation effects. In fact they cannot be due to local variations of the g tensors, which are expected to be isotropic and very close to the free electron value for both the manganese and the radicals.

Short-range order effects in EPR spectra were first observed by Nagata and Tazuke²⁵ in the antiferromagnetic linear chains $(\text{CH}_3)_4\text{NMnCl}_3$ (TMMC) and $\text{CsMnCl}_3 \cdot 2\text{H}_2\text{O}$ (CMC). For ideal one-dimensional materials at low temperature the exchange interaction tends to keep the spins correlated and the dipolar interaction within the chain determines the preferred spin orientations. As a consequence the magnetic susceptibility of the chains depends on the orientation of the external magnetic field even if it is isotropic in the high-temperature limit. The anisotropy of the susceptibility affects an EPR experiment: the resonance field must be smaller than in the high-temperature limit along a direction that has susceptibility higher than the isotropic value and larger in a direction of smaller susceptibility. As a consequence the effective g values became anisotropic and temperature dependent. In $\text{Mn}(\text{hfac})_2\text{NIT-}i\text{-Pr}$ the g shifts are quasi-axial and

(21) Seiden, J. J. *Phys., Lett.* **1983**, *44*, L947.

(22) Unpublished results of the Florence laboratory.

(23) Renard, J. P. In *Organic and Inorganic Low Dimensional Crystalline Materials*; Delhaes, P., Drillon, M., Eds.; NATO ASI Series; Plenum: New York, 1987; p 125.

(24) Villain, J.; Loveluck, J. M. *J. Phys., Lett.* **1977**, *38*, L77.

(25) Nagata, K.; Tazuke, Y. *J. Phys. Soc. Jpn.* **1972**, *32*, 337.

negative along the chain, while the reverse pattern with positive g shift along the chain was previously observed in typical one-dimensional antiferro- and ferromagnets.^{25,30,31} We want to stress here that this behavior is indeed typical of ideal ferrimagnetic chains. In fact, the preferred spin orientation in one-dimensional materials is determined by both dipolar and exchange interactions between nearest neighbors. For a ferromagnetic chain the spins orient parallel to each other along the chain (Figure 6a) and the g tensor has a positive shift along this direction. When the intrachain exchange is antiferromagnetic, the preferred spin orientation is orthogonal to the chain, as shown in Figure 6b: for an antiferromagnet the direction along which the spins are preferentially oriented corresponds to the smallest susceptibility value, due to the cancellation of the moments, but for a ferrimagnet this direction corresponds to a maximum in susceptibility because the different moments do not cancel.

A quantitative analysis of the temperature dependence of the resonance field was performed by Nagata and Tazuke²⁵ extending the Fisher classical spin model²⁶ in the assumption of uniaxial symmetry along the chain direction. The method applies equally well to ferro- and antiferromagnetic one-dimensional materials.

To the best of our knowledge, up to now no extension to the case of alternating spins, e.g. to ferrimagnetic chains, has been performed. Analogous effects were observed in 1-D ferrimagnets formed by copper(II)-manganese(II) chains, but no quantitative analysis was possible in that case because the strongest dipolar interaction is not intra- but interchain in nature.²⁷ In the present case the dipolar interaction is strongest between nearest neighbors along the chain, so that the Nagata and Tazuke formalism should be easily extended.

The resonance frequencies parallel and perpendicular to the chain direction are related to the anisotropic susceptibility by the relations^{28,29}

$$h\omega_{\parallel} = g\mu_B H \frac{\chi_{\parallel}}{\chi^{\perp}} \quad h\omega_{\perp} = g\mu_B H \left(\frac{\chi^{\perp}}{\chi_{\parallel}} \right)^{1/2} \quad (1)$$

The susceptibility can be written as

$$\chi^{\alpha} = \chi_0 - D\chi^{\alpha}_a \quad (2)$$

where χ_0 is the isotropic susceptibility of a linear chain calculated by using the Fisher procedure,²⁶ χ^{α}_a is the anisotropic contribution arising from the dipolar interaction, D is the parameter of dipolar interaction (in K), which in the point dipolar approximation corresponds to μ_B^2/r^3 , r being the distance between the spins, and α can be \perp or \parallel , meaning perpendicular or parallel to the chain direction. The susceptibilities are the same as we observe in our magnetic anisotropy experiments, and indeed the two techniques provide the same type of information.

The dipolar contribution to the susceptibility can be evaluated by the summation of four-spin correlation functions:

$$\sum_{m=0}^N \sum_{n=0}^N \sum_{j=1}^N g_m g_n (S_m^{\alpha} S_n^{\alpha} (2S_j^{\perp} S_{j-1}^{\perp} - 2S_j^{\parallel} S_{j-1}^{\parallel}))_{H=0} / (N+1)$$

In order to take into account the presence of alternating spins, we divided the summation in two parts. The terms with $m-n$ even must be multiplied by the factor $g_A^2 + g_B^2$, because identical spins are involved, while those with $m-n$ odd must be multiplied by $2g_A g_B$, where g_A and g_B refer to the spins of type A and B,

respectively. The results can be summarized as

$$\chi_0 = \frac{N\mu_B^2}{3kT} \left[G^2 \frac{1+u}{1-u} + \Delta G^2 \frac{1-u}{1+u} \right] \quad (3)$$

$$\chi^{\perp}_a = \frac{Ng_A g_B S_A S_B \mu_B^2}{kT^2} \left[\frac{2}{15} \left[2 - \frac{u}{K} \right] \times \left[\frac{G^2}{(1-u)^2} - \frac{\Delta G^2}{(1+u)^2} \right] + \frac{4}{45} K \left[G^2 \frac{1+u}{1-u} - \Delta G^2 \frac{1-u}{1+u} \right] \right] \quad (4)$$

$$\chi^{\parallel}_a = -2\chi^{\perp}_a$$

with

$$K = \frac{J(S_A(S_A+1)S_B(S_B+1))^{1/2}}{kT}$$

$$u(K) = \coth K - 1/K$$

$$G^2 = \frac{1}{2} [g_A(S_A(S_A+1))^{1/2} + g_B(S_B(S_B+1))^{1/2}]$$

$$\Delta G^2 = \frac{1}{2} [g_A(S_A(S_A+1))^{1/2} - g_B(S_B(S_B+1))^{1/2}]$$

It is easy to verify that (4) reduces to the Nagata-Tazuke expression²⁵ for $\Delta G = 0$, i.e. if the two moments are identical. Using (1), with J fixed at the value obtained from the analysis of the magnetic susceptibility using the classical Fisher model, $J = 313 \text{ cm}^{-1}$,²⁶ and $D = 0.06 \text{ K}$, we calculated the curve in Figure 2. The general trend is reproduced, although our assumptions do not take into account the actual rhombic symmetry of the system. Further, the presence of the spin $S = 1/2$, which can be hardly treated as a classical vector, and of single-ion anisotropy, which may not be negligible, represent other limitations of our simple model. However, notwithstanding these drawbacks it seems to work fairly well. The successful fitting of the resonance fields confirms that the interaction within the chain is antiferromagnetic. We reached the same conclusion from the analysis of the magnetic susceptibility,¹⁸ but a margin of uncertainty was left, that now is completely removed.

The temperature dependence of the EPR line width and line shape in one-dimensional systems is not yet fully understood. Again a relatively simple treatment due to Tazuke and Nagata³² explicitly considers the diffusive (important at high temperature) and Gaussian (important at low T) contributions to the line shape and line width. In fact the EPR absorption is determined by the time evolution of the total-spin correlation function, ψ , whose behavior is Gaussian at short times ($\tau < \tau_1 = 2/\omega_e$, where ω_e is the exchange frequency) and diffusive at long times ($\tau > \tau_1$). The ψ function can be written as

$$\psi = \psi_G + \psi_D$$

where ψ_G and ψ_D are the Gaussian and diffusive parts, respectively. At high temperature ψ_D dominates and the EPR line is intermediate between Lorentzian and Gaussian at $\theta = 0^\circ$, while the line width follows a $(3 \cos^2 \theta - 1)^{4/3}$ angular dependence. When the temperature is lowered, the Gaussian component increases and the diffusive component decreases until eventually the line shape becomes Lorentzian at all angular settings and the line width follows a $1 + \cos^2 \theta$ angular dependence. The line width increases on decreasing temperature.

Our experimental results follow nicely these predictions, the line shape going closer to the Lorentzian limit at low temperature, as shown in Figure 4, and the line width increasing on decreasing temperature and losing the magic-angle behavior. If the qualitative behavior is satisfactory, a quantitative fitting appears more problematic, because the observed line width enhancement is very anisotropic, the values observed parallel to the chain direction increasing much faster than those orthogonal to it. We have no

(26) Fisher, M. E. *Am. J. Phys.* **1964**, *32*, 343.

(27) Gatteschi, D.; Guillo, O.; Zanchini, C.; Sessoli, R.; Kahn, O.; Verdager, M.; Pei, Y. *Inorg. Chem.* **1989**, *28*, 287.

(28) Oshima, K.; Okuda, K.; Date, M. *J. Phys. Soc. Jpn.* **1976**, *41*, 475.

(29) Karasudani, T.; Okamoto, H. *J. Phys. Soc. Jpn.* **1977**, *43*, 1131.

(30) Caneschi, A.; Gatteschi, D.; Rey, P.; Zanchini, C. *J. Chem. Soc., Faraday Trans.* **1987**, *83*, 3603.

(31) Bencini, A.; Gatteschi, D. In *EPR of Exchange Coupled Systems*; Springer-Verlag: West Berlin, in press.

(32) Tazuke, Y.; Nagata, K. *J. Phys. Soc. Jpn.* **1975**, *38*, 1003.

rationale to offer for this at the moment, and more experimental data are needed before any conclusion can be reached.

The present results show that the manganese-radical chains are well suited for yielding bulk magnetic materials, because, even if the interchain interactions are weak and mainly dipolar in nature, the strong intrachain coupling gives a high correlation at low temperature enhancing the interchain interaction. In order

to reach the goal to increase the transition temperature, it will be necessary to pass from one dimension to two or three dimensions involving directly the metal ions and the radicals or to create interchain exchange pathways either by using appropriate coligands or by introducing suitable substituents on the radicals.

Registry No. Mn(hfac)₂NIT-*i*-Pr, 113547-95-8.

Contribution from the Institute for Inorganic Chemistry, University of Witten/Herdecke, Stockumerstrasse 10, 5810 Witten, Federal Republic of Germany

Kinetics and Mechanism of the Ligand Substitution Reactions of *N*-(Hydroxyethyl)ethylenediaminetriacetate Complexes of Ruthenium(III) in Aqueous Solution

H. C. Bajaj¹ and R. van Eldik*

Received October 12, 1988

The kinetics of the substitution reactions of Ru(hedtra)H₂O (hedtra = *N*-(hydroxyethyl)ethylenediaminetriacetate) with SCN⁻, N₃⁻, thiourea, and substituted thiourea were studied as a function of pH (2-8), temperature (20-45 °C), and pressure (0.1-100 MPa). The observed rate constants exhibit a characteristic decrease with increasing pH in the range 3.5-6 but remain constant in the ranges 2-3.5 and 6-8.5. The activation parameters measured in the pH-independent regions fall in the ranges $34 \leq \Delta H^\ddagger < 40$ kJ mol⁻¹, $-108 \leq \Delta S^\ddagger \leq -92$ J K⁻¹ mol⁻¹, and $-14 \leq \Delta V^\ddagger \leq -4$ cm³ mol⁻¹ and support the operation of an associatively activated ligand substitution process. The results are discussed in reference to data for the corresponding ethylenediamine-tetraacetate complexes and in terms of the labilization effect of such chelate ligands.

Introduction

We recently reported a detailed kinetic and mechanistic study of the substitution behavior of ethylenediaminetetraacetate complexes of Ru(III) with a series of anionic and neutral ligands in aqueous solution.² In general, these complexes exhibit a remarkable lability in comparison to other nonchelated complexes of Ru(III).^{3,4} A maximum reactivity is reached at $4 < \text{pH} < 6$, which is ascribed to the participation of the very labile Ru-(edta)H₂O⁻ species, although the reason for this effect remains unresolved.^{2,5-7} We concluded² that hydrogen bonding between the free carboxylate oxygen and the coordinated water molecule must account for the high lability of the water molecule. This can either result in the creation of an open area and accessible site for associative substitution or labilize the water molecule directly by affecting the metal-oxygen bond strength.⁵

In an effort to gain more insight into the intimate nature of this catalytic effect, we are presently investigating the influence of the nature of the pendant group in a series of Ru^{III}(L)H₂O complexes, where L denotes *N*-substituted ethylenediaminetriacetate. Ogino and co-workers demonstrated that the transient coordination of the pendant group plays an important role in the unexpected rapid substitution reactions of the corresponding Cr(III) complexes.⁷⁻⁹ In this paper we report our results for the substitution of Ru(hedtra)H₂O by SCN⁻, N₃⁻, SC(NH₂)₂, SC(NHMe)₂, and SC(NMe)₂, where hedtra = *N*-(hydroxyethyl)ethylenediaminetriacetate. This complex is substantially less labile than the Ru(edta)H₂O⁻ complex and demonstrates the important

effect of the pendant carboxylate group in the latter case.

Experimental Section

Materials. K[Ru(hedtra)Cl] was prepared from K₂[RuCl₅(H₂O)] in the following way: To 0.5 g (1.33 mmol) of K₂[RuCl₅(H₂O)] in 10 mL of 0.001 M HClO₄ was added 0.506 g (1.33 mmol) of Na₃hedtra in 15 mL of 0.001 M HClO₄. The solution was refluxed for ca. 2 h, followed by evaporation on a water bath to a small volume and addition of ethanol, which produced a greenish yellow precipitate. The latter was filtered off, washed with a cold water-ethanol (1:9) mixture, and dried in a desiccator. Anal.¹⁰ Found (calcd): C, 26.6 (26.6); H, 4.3 (3.4); N, 6.5 (6.2). All other chemicals used were of analytical reagent grade, and deionized water was used to prepare all solutions. Acetate-acetic acid, borate, and phosphate buffers were used to maintain a constant pH. The ionic strength of the solutions was adjusted with Na₂SO₄.

Instrumentation. Substitution reactions were followed spectrophotometrically by using a Shimadzu UV 250 spectrophotometer and a Durum D110 stopped-flow instrument. Kinetic measurements at elevated pressure (up to 100 MPa) were performed on a homemade high-pressure stopped-flow unit.¹¹ All the instruments used for the kinetic measurements were thermostated to ± 0.1 °C. The absorbance-time plots were analyzed with the aid of a data acquisition system,¹² and the corresponding first-order plots were linear for at least 2-3 half-lives of the reaction. pH measurements were carried out with a Radiometer PHM 64 instrument.

Results and Discussion

The K[Ru(hedtra)Cl] complex was characterized by elemental analyses and IR data. It exhibits a characteristic band at 1632 cm⁻¹ due to the coordination of carboxylate to the Ru center. This complex hydrolyzes rapidly on dissolution to produce the Ru(hedtra)H₂O species, which exhibits a maximum absorbance at 285 nm. This peak shifts to 330 nm on increasing the pH (see Figure 1) with an isosbestic point at 312 nm due to the formation of the Ru(hedtra)OH⁻ species. Similar spectral changes have also been reported for the deprotonation of Cr(hedtra)H₂O and Cr-

- (1) On leave from the Central Salt and Marine Chemicals Research Institute, Gijubhai Badheka Marg., Bhavnagar 364002, India.
- (2) Bajaj, H. C.; van Eldik, R. *Inorg. Chem.* **1988**, *27*, 4052.
- (3) Taube, H. *Comments Inorg. Chem.* **1981**, *1*, 17 and references cited therein.
- (4) Rapaport, I.; Helm, L.; Merbach, A. E.; Bernhard, P.; Ludi, A. *Inorg. Chem.* **1988**, *27*, 873.
- (5) Matsubara, T.; Creutz, C. *Inorg. Chem.* **1979**, *18*, 1956.
- (6) Toma, H. E.; Santos, P. S.; Mattioli, M. P. D.; Oliveira, L. A. A. *Polyhedron* **1987**, *6*, 603.
- (7) Ogino, H.; Shimura, M. *Adv. Inorg. Bioinorg. Mech.* **1986**, *4*, 107.
- (8) Ogino, H.; Watanabe, T.; Tanaka, N. *Inorg. Chem.* **1975**, *14*, 2093.
- (9) Ogino, H.; Shimura, M.; Tanaka, N. *Inorg. Chem.* **1979**, *18*, 2497.

- (10) Beller Analytical Laboratory, Göttingen, FRG.
- (11) van Eldik, R.; Palmer, D. A.; Schmidt, R.; Kelm, H. *Inorg. Chim. Acta* **1981**, *50*, 131.
- (12) Kraft, J.; Wieland, S.; Kraft, U.; van Eldik, R. *GIT Fachz. Lab.* **1987**, *31*, 560.